RSC Advances

PAPER

View Article Online
View Journal | View Issue



Cite this: *RSC Adv.*, 2017, **7**, 18136

# Nanoarchitectures by hierarchical self-assembly of ursolic acid: entrapment and release of fluorophores including anticancer drug doxorubicin†

Braja Gopal Bag,* Subhajit Das, Sk Nurul Hasan and Abir Chandan Barai

Received 20th February 2017
Accepted 13th March 2017

DOI: 10.1039/c7ra02123b

rsc.li/rsc-advances

Ursolic acid, a naturally occurring 6-6-6-6-6 monohydroxytriterpenic acid, is extractable from the leaves of *Plumeria rubra*. In continuation of our ongoing efforts on the studies of the self-assembly properties of naturally occurring triterpenoids, herein, we report our detailed investigation on the self-assembly of this ursane type triterpenic acid in different liquids. The molecule self-assembles in most organic as well as aqueous organic liquids yielding nano-architectures such as vesicles, tubes, fibers and flowers affording supramolecular gels in many of the liquids studied. Characterization of the self-assemblies has been carried out using atomic force microscopy, scanning electron microscopy, transmission electron microscopy, optical microscopy, dynamic light scattering, FTIR and X-ray diffraction studies. The self-assemblies have been utilized for the entrapment of fluorophores including an anticancer drug, doxorubicin. Release of the entrapped fluorophores including doxorubicin has been demonstrated at physiological pH as well as lower pH values.



## 1. Introduction

Molecular self-assembly, a process by which molecules spontaneously assemble in a medium to form an ordered structure yielding supramolecular architectures *via* non-covalent forces such as hydrogen bonding, electrostatic, van der Waals, aromatic–aromatic, and solvophobic interactions, has been an area of intense research during the last decade.[1–5] The supramolecular architectures formed by the self-assembly of small molecules yielding fibers, vesicles, spheres, tubes and porous microstructures have found interesting applications in drug delivery,[6,7] tissue engineering,[8] pollutant capture,[9] templating nanomaterials, *etc.* Self-assembly properties of different classes of compounds such as proteins and peptides,[10–12] fatty acids,[13–15] sophorolipids,[16,17] steroids,[18] sugars,[19,20] *etc.* have been reported. Investigations on the utilization of plant derived chemicals have gained renewed interest in recent years, because of their renewable nature, biocompatibility and easy availability from nature without multistep synthetic efforts. Among various plant secondary metabolites, triterpenoids, the C30 subset of the major plant secondary metabolite terpenoids, have recently been recognized as renewable functional nano-entities in supramolecular chemistry and nanoscience.[21] Inspite of the abundance of hundreds of triterpenoids, having diversified skeletons with one or more amended hydroxy or carboxy groups in common, there are only a few examples in the literature on the self-assembly of triterpenoids.[4] The examples of the self-assembly of molecules without functional modifications are not common.[22] Recently, we have reported the self-assembly properties of the triterpenoids betulinic acid,[23] betulin,[24] oleanolic acid,[25] glycyrrhetinic acid[26] and arjunolic acid[27] in different liquids and observed that, minute structural variation in the triterpenoid back-bone and functional group dispositions resulted in drastic changes in their self-assembly properties.

Ursolic acid, a 6-6-6-6-6 pentacyclic monohydroxy triterpenic acid, is extractable from the leaves of *Plumeria rubra* as a free acid having wide varieties of pharmacological activities (Fig. 1).[28–32] Anticancer and antitumor activities of ursolic acid have been reported in different cell lines.[33–36] It is identical to oleanolic acid (Fig. S2 ESI†) having identical backbone and functional groups except the 29-$CH_3$ and 30-$CH_3$ groups which are geminal (at C20) in oleanolic acid and vicinal (at C19 and C20) in ursolic acid. Occurrence of the pentacyclic triterpenoids having a β-amyrin (oleanane) skeleton along with α-amyrins (ursane) is common in nature and has been explained by 1,2-$CH_3$ migration during their biosynthesis.[37,38] Mostly vesicular self-assembly along with certain percentage of fibrillar network of oleanolic acid have been reported by us.[24] In continuation of the previous reports from our laboratory that minute variation in the triterpenoid skeleton or functional group disposition can have profound effect on the self-assembly properties in different

*Department of Chemistry and Chemical Technology, Vidyasagar University, Midnapore 721102, West Bengal, India. E-mail: braja@mail.vidyasagar.ac.in*

† Electronic supplementary information (ESI) available. See DOI: 10.1039/c7ra02123b

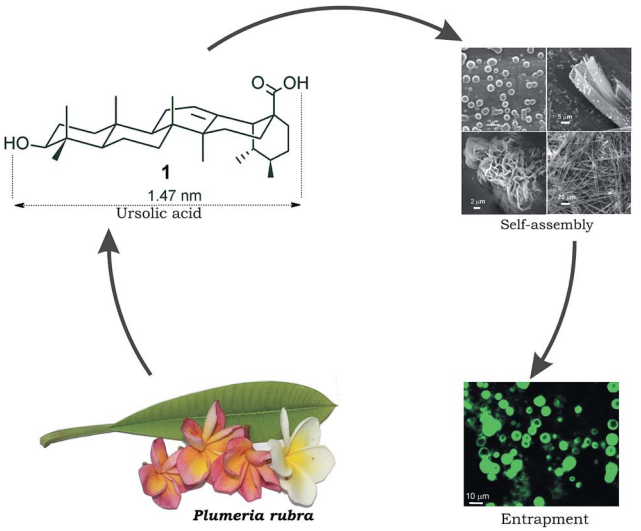


Fig. 1 Schematic representation of self-assembly of ursolic acid **1** extractable from *Plumeria rubra* yielding nano-architectures and its use in drug entrapment.

liquids, it occurred to us that ursolic acid **1**, extractable from the leaves of *Plumeria rubra* will be an interesting molecule for the study of its self-assembly properties in different liquids. Herein we report that ursolic acid self-assembles in different neat liquids as well as aqueous liquid mixtures yielding supramolecular architectures such vesicles, tubes, fibers and flowers of nano- to micro-meter dimensions. The vesicular self-assemblies are capable of entrapping fluorophores including the anticancer drug doxorubicin. Release studies of the entrapped fluorophores including the anticancer drug doxorubicin has also been demonstrated making it useful as a drug delivery vehicle.

## 2. Results and discussion

### 2.1 Study of self-assembly properties

Ursolic acid was extracted from the leaves of *Plumeria rubra* and purified by an improved method developed in our laboratory (see Experimental section). Self-assembly studies of ursolic acid were carried out in different organic liquids, as well as aqueous solvents such as ethanol–water, DMSO–water and DMF–water. In the case of neat liquids, a weighed amount of ursolic acid (usually 5 mg) was dissolved in the liquid contained in a vial under hot condition and then the resulting solution was allowed to cool at room temperature. If the material did not flow under gravity as observed by turning the vial upside down, we called it a gel. In the case of mixed solvents, ursolic acid was initially solubilized in the organic liquid under hot condition and then water was added gradually till cloudiness appeared. Then the mixture was re-dissolved by heating and the clear solution thus obtained was allowed to cool at room temperature and examined as before. Among the 22 neat organic liquids tested for the self-assembly studies, ursolic acid self-assembled in most of the liquids in the concentration range of 1–6% w/v forming gels in 12 neat liquids (Tables 1 and TS1, ESI†). Among the three aqueous liquid mixtures tested for the self-assembly studies, ursolic acid self-assembled in all the aqueous liquids forming a strong gel in DMSO–water (Table TS2 ESI†).

Table 1 Results of the self-assembly studies of ursolic acid **1**[c]

| Entry | Solvent | State[a] | MGC | $T_{gel}$[b] (°C) |
|---|---|---|---|---|
| 1 | Toluene | CS | 2.0 | — |
| 2 | *o*-Xylene | G | 1.64 | 35.1 |
| 3 | *m*-Xylene | G | 1.04 | 33.2 |
| 4 | Mesitylene | G | 1.41 | 63.2 |
| 5 | Chloro benzene | G | 4.01 | 57 |
| 6 | *o*-Dichloro benzene | G | 1.0 | 37.4 |
| 7 | Isopropanol | C | 2.0 | — |
| 8 | Ethylene glycol | CS | 1.33 | — |

[a] CS = colloidal suspension, G = gel, C = crystal; concentrations are in % w/v. [b] Gel to sol transition temperatures ($T_{gel}$) are provided at minimum gelator concentration MGC. [c] See Table TS1 ESI for a complete table.

### 2.2 Morphological characteristics of the self-assemblies

The morphology of the self-assemblies were studied by atomic force microscopy (AFM), scanning electron microscopy (SEM), high resolution transmission electron microscopy (HRTEM), optical microscopy, dynamic light scattering (DLS), FTIR and XRD studies. Atomic force microscopy of the dried self-assemblies of **1** (Fig. 2 and S3 ESI†) prepared from a solution of **1** in ethanol–water (3 : 1, 0.12% w/v) indicated the formation of spherical self-assemblies of 120–360 nm diameters and heights 23–27 nm (calculated from the diameters of 149 spheres, Fig. S4, ESI†). The 3D images clearly indicated the spherical nature of the self-assemblies. The measured heights do not match with radius of the spherical objects due to deformation by the AFM tip indicating a soft nature of the spherical self-assemblies. SEM studies with the dried self-assemblies of **1** prepared from a colloidal suspension in ethanol–water (3 : 1, 0.23% w/v) indicated poly-disperse spherical self-assemblies of nano- to micrometer diameters (average size of 480 nm calculated from 87 spherical self-assemblies, Fig. 3a). Tubular self-assemblies along with spherical self-assemblies were observed in SEM images of the dried self-assemblies of **1** prepared from a solution in ethanol–water at 0.23% w/v along with certain percentage of fibrillar network (Fig. 3b and S5 ESI†). HRTEM images of the spherical self-assemblies clearly indicated the vesicular nature of spherical self-assemblies (Fig. 3c and S6 ESI†). With the membrane thickness of 2.94 nm and the molecular length being 1.47 nm, a bilayer vesicular structure is proposed (Fig. 3d). The membrane thickness of the nano-tubes observed by HRTEM was also 2.94 nm (Fig. 3e) supporting bilayer morphology of the tubular self-assemblies (Fig. 3f). The bilayer membrane morphology is supported by X-ray diffraction studies of a gel of **1** in *m*-xylene (2.1% w/v) that revealed a sharp peak at $2\theta = 3.0$, which corresponds to a *d* spacing of 2.94 nm.

Spherical objects of 360–654 nm diameters (calculated from 70 spherical objects) were observed in the SEM images of the self-assemblies of **1** prepared from a solution in *m*-xylene

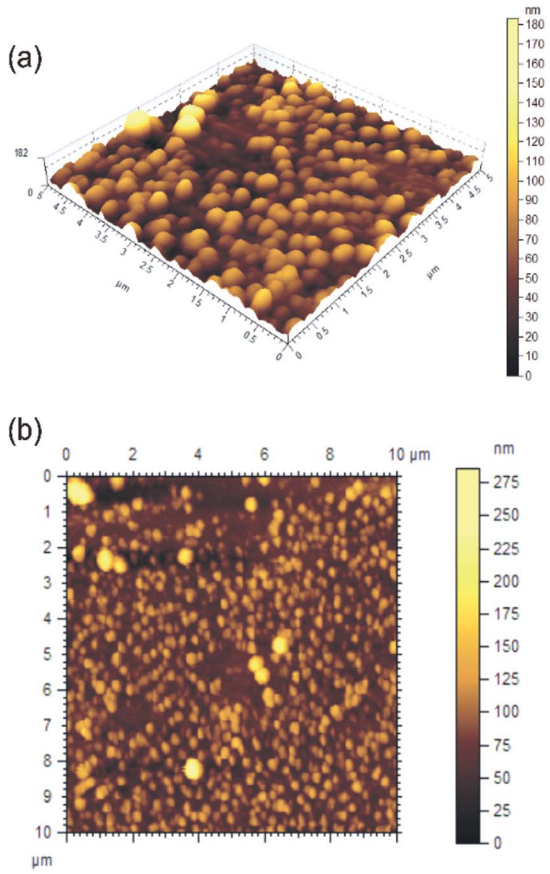


Fig. 2 AFM images ((a) 3D, (b) 2D) of the self-assemblies of ursolic acid in ethanol–water (3 : 1. 0.11% w/v).

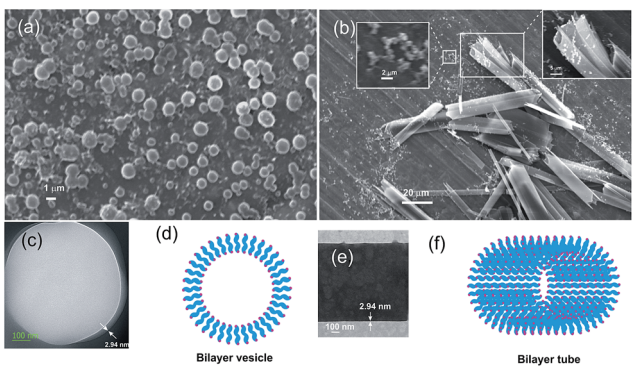


Fig. 3 (a and b) Scanning electron micrographs of the dried self-assemblies of ursolic acid prepared from colloidal suspension in ethanol–water (3 : 1): (a and b) 0.23% w/v, (c) HRTEM (unstained) of self-assembled ursolic acid in mesitylene (0.21% w/v), (d) model bilayer vesicle, (e) tube in ethanol–water (3 : 1), (f) model tube.

(0.23% w/v) (Fig. 4a and b and S7 ESI†). Densely packed spherical self-assemblies along with micro-sized flowers were observed at a higher concentration (0.52–1.0% w/v) of **1** in *m*-xylene. Such spherical self-assemblies along with flowers were observed in the dried samples prepared from toluene, mesitylene and chlorobenzene (Fig. S8 and S9 ESI†).

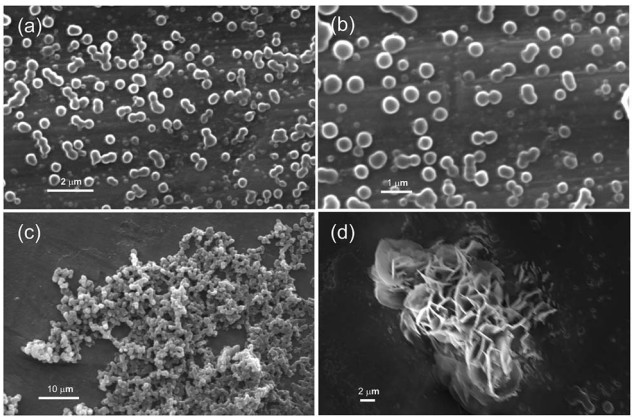


Fig. 4 (a–d) Scanning electron micrographs of the dried self-assemblies of ursolic acid prepared from dilute solution in *m*-xylene: (a and b) 0.23% w/v, (c) 1.0% w/v; (d) 0.52% w/v.

To measure the hydrodynamic diameter of the self-assemblies of **1**, DLS studies were carried out in chlorobenzene (0.2% w/v), *o*-dichlorobenzene (0.16% w/v), mesitylene (0.21% w/v) and ethanol–water (0.23% w/v), (Fig. S10 ESI†). In all the cases studied, polydisperse self-assemblies of mostly nano-metric dimensions were observed. For example, in ethanol–water (0.23% w/v), most of the assemblies were of size 182 nm. In *o*-dichlorobenzene (0.16% w/v), the assemblies had size in the range of 63–518 nm. In mesitylene (0.21% w/v) the average size of the self-assemblies was 900 nm. In chloro benzene (0.2% w/v), most of the assemblies were of size 2.1 μm. These studies revealed that mostly nano-sized assemblies along with certain percentage of micro-sized assemblies were formed in all the liquids studied which are in consistent with the results from AFM, SEM and HRTEM studies. Hydrodynamic diameters measured for the self-assemblies in DMSO–water at different time intervals after sonication shed light into the growth of the self-assemblies (Fig. S11, ESI†).

Formation of vesicular self-assemblies at a lower concentration of **1** which form densely packed vesicular self-assemblies at a higher concentration, as observed in the xero-gels of **1** by SEM (discussed previously), prompted us to propose a mechanism for the formation of gel *via* vesicular self-assemblies (Fig. 5). With increasing concentration of **1** the viscosity of the solutions increased due to immobilization of the liquid by the interconnected and densely packed vesicles yielding a gel above its MGC. Formation of gels *via* vesicular self-assemblies, though not very common, has been reported by us previously on monohydroxy and trihydroxy triterpenoids and by others on synthetic supramolecular systems.[24,25,39,40] Encapsulation of various types of molecules including fluorophores including drugs can provide opportunities for drug delivery and related application which has been discussed in Section 2.3. Observation of bilayer vesicular self-assemblies along with bilayer tubes in ethanol–water by HRTEM prompted us to propose a mechanism for the formation of bilayer tube formation along with bilayer vesicles (Fig. 5). Thicker membrane of tubes observed by SEM (Fig. 3b) might be due to multilamellar membrane morphology. Such tubular self-assemblies along with vesicular

 

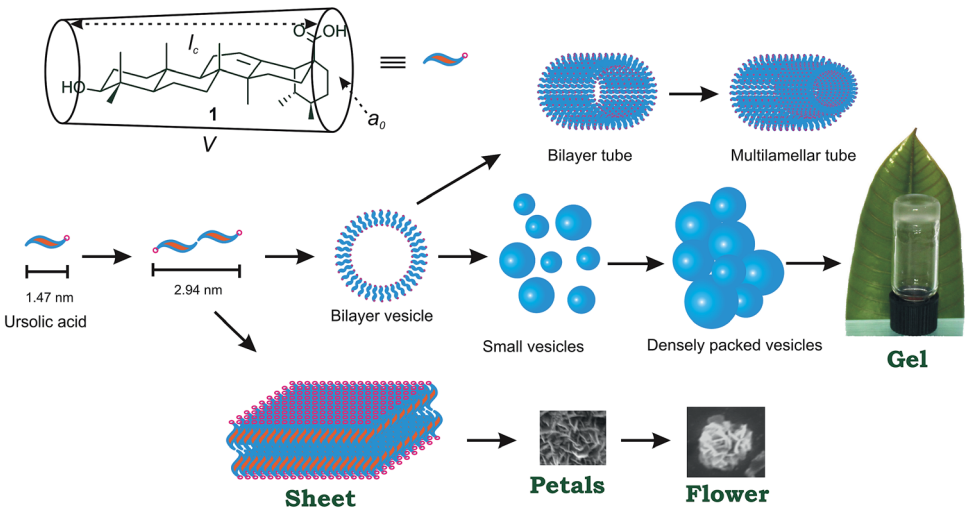


Fig. 5 Schematic representation of hierarchical self-assembly of ursolic acid yielding vesicles, tubes and flowers. Inverted vial shows a supramolecular gel with the leaf of *Plumeria rubra* in the background.

self-assemblies though not very common, have been reported on a few synthetic supramolecular systems.[41]

A very fine balance of the hydrophobic and hydrophilic forces play a role during self-assembly of amphiphiles in liquids and different morphologies may result which may not be at thermodynamic equilibrium. Formation of different morphologies has been explained based on packing parameter $P = V/a_0 l_c$ where $V$ and $l_c$ are the volume and the length of the hydrophobic part and $a_0$ is the cross-sectional area of the hydrophilic part of the amphiphile (Fig. 5).[42] Bilayers with a spontaneous curvature may result when $1/2 < P < 1$ is met (Fig. 5) yielding vesicles and tubes. Two dimensional assembly of the amphiphiles can produce a sheet or petal morphology which can undergo hierarchical self-assembly producing flowers. H-Bonding involving the hydroxyl and the carboxyl groups in addition to the dispersion interactions by the triterpenoid backbones are likely to have played a significant role for the self-assembly of the molecules. The stretching frequency of the 'O–H' group in the neat powder appeared at 3415 $cm^{-1}$ whereas the 'O–H' stretching frequencies of the dried self-assemblies prepared from 2-propanol, *o*-dichlorobenzene and bromobenzene appeared at 3353, 3312, and 3412 $cm^{-1}$ respectively (Fig. S12 ESI†). Similarly, the stretching frequency of the 'C=O' group in the neat powder appeared at 1693 $cm^{-1}$ whereas the 'C=O' stretching frequencies of the dried self-assemblies prepared from 2-propanol, *o*-dichlorobenzene and bromobenzene appeared at 1652, 1659, and 1689 $cm^{-1}$ respectively. The shifting in the "–O–H" and "–C=O" stretching frequencies in the self-assemblies compared to the neat powder clearly indicated that the self-assemblies were stabilized by the intermolecular H-bonding among the molecules.

### 2.3 Thermo-reversibility and thermodynamic parameters

All the gels were thermo-reversible. Hence the gel to sol transition temperature $T_{gel}$ were plotted against the % gelator concentration. With increase in the concentration of the gelator the $T_{gel}$ increased indicating stronger intermolecular interactions and increased branching at higher concentrations. The $T_{gel}$ value for the *o*-dichlorobenzene gel at its minimum gelator concentration (MGC) (1% w/v) was 37.4 °C and increased to 71.1 °C (Fig. 6a) at 4% (w/v) concentration. Similarly, the $T_{gel}$ value of the *m*-xylene gel at MGC (1.04% w/v) was 33.2 °C and increased to 66 °C (Fig. 6b) at 3.28% (w/v) concentration. Similarly, the $T_{gel}$ value of the DMSO–$H_2O$ gel at MGC (2.12% w/v) was 41.2 °C and increased to 72.6 °C (Fig. 6c) at 8.5% (w/v) concentration. Increase of $T_{gel}$ with concentration allowed us to calculate the thermodynamic parameters ($\Delta H^o$, $\Delta S^o$, $\Delta G^o$) at 298 K (Table 2).

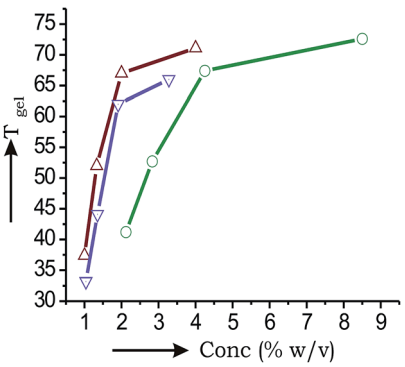


Fig. 6 Plots of $T_{gel}$ *vs.* concentration for **1** in: (a) *o*-dichlorobenzene (-Δ-); (b) *m*-xylene (-∇-); (c) DMSO–$H_2O$ (-○-).

Table 2 Thermodynamic parameters ($\Delta H^o$, $\Delta S^o$, $\Delta G^o$) for gel to sol transition of gels of ursolic acid **1** in different liquids at 298 K

| Liquid | $\Delta H^o$ kJ $mol^{-1}$ | $\Delta S^o$ J $mol^{-1}$ $K^{-1}$ | $\Delta G^o$ kJ $mol^{-1}$ |
|---|---|---|---|
| *m*-Xylene | 27.56 | 52.34 | 14.75 |
| *o*-Dichlorobenzene | 22.77 | 48.21 | 12.34 |
| DMSO–water | 25.84 | 51.29 | 10.45 |

The positive free energy changes ($\Delta G^{o}$) during gel to sol transformations in all the cases indicated the stability of the gels.

### 2.4 Study of entrapment of fluorophores including anticancer drug doxorubicin

Development of biocompatible nano carriers has been an emerging area of research for efficient and targeted drug delivery with an aim to minimize the serious side-effects in chemotherapy.[43–46] Optical microscopy of the self-assemblies of **1** in DMF–water (5 : 1, 3.5% w/v) revealed micro-sized vesicular self-assemblies (Fig. S13 ESI†). This prompted us in studying the entrapment of guest molecules inside the self-assemblies.

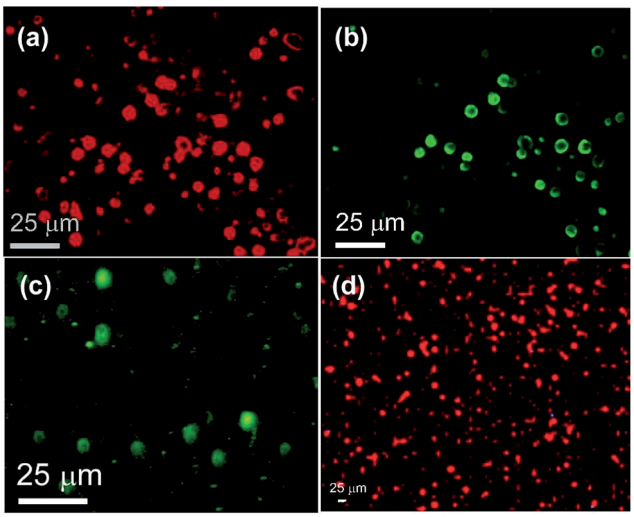


Fig. 7 Epifluorescent microscopy images of self-assembled ursolic acid (a–c) in ethanol–water (3 : 1, 30.13 mM): (a) containing Rhodamine-B (0.30 mM) exposed under green emission light, (b) containing Rhodamine-B (0.30 mM) exposed under blue emission light, (c) containing CF (0.30 mM) exposed under blue emission light, (d) in ethanol–water (3 : 1, 22.93 mM) containing doxorubicin (2.2 mM) exposed under green emission light.

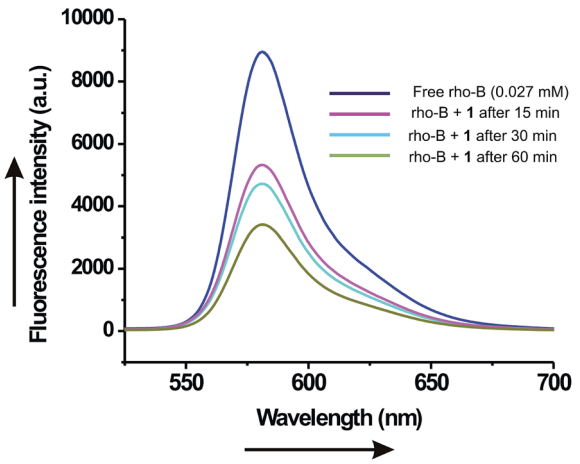


Fig. 8 Fluorescence emission spectra ($\lambda_{ex}$ = 510 nm) of free Rho-B and encapsulated Rho-B inside the vesicular self-assemblies of ursolic acid at different time intervals.

Whether the vesicular self-assemblies of **1** are capable of entrapping drug molecules, we initially examined the entrapment of the cationic dye Rhodamine B (Rho-B) and the anionic dye 5,6-carboxyfluorescein (CF). To our delight, we observed that the vesicular self-assemblies were capable of entrapping both the fluorophores. For example, when a hot solution of ursolic acid in ethanol–water (3 : 1, 30.13 mM) containing Rho-B (0.30 mM) was cooled at room temperature and examined by epifluorescence microscopy, bright fluorescence from the vesicular self-assemblies indicated the entrapment of fluorophores inside the vesicles (Fig. 7a and b).

Encapsulation of Rho-B was further supported from the comparative fluorescence intensity of the free Rho-B and entrapped Rho-B in vesicles at 582 nm ($\lambda_{ex}$ = 510 nm) (Fig. 8). Reduction in fluorescence intensity of vesicle entrapped Rho-B with time compared to that of free Rho-B was observed. This might be due to its self-quenching property under confined conditions.[47–49] The vesicular nature of the fluorophore-loaded self-assemblies remained intact even after removal of the

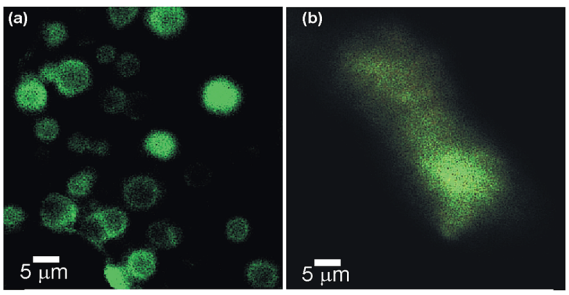


Fig. 9 Epifluorescence microscopy images of Rho-B loaded self-assemblies of ursolic acid in DMSO–water (5 : 3): (a) before and (b) after the treatment of Triton-X 100.

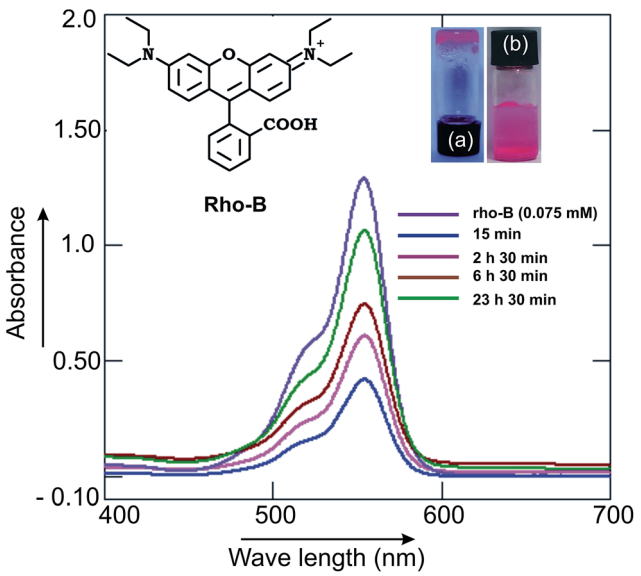


Fig. 10 Release of the ursolic acid (55 mM) gel-entrapped fluorophore Rho-B (0.54 mM): overlay of the UV-visible spectra of the released Rho-B to buffers at pH 7.2 at various time intervals.

liquids as observed by SEM carried out with the fluorophore-loaded self-assemblies (Fig. S14, ESI†).

Triton X-100 is a well known nonionic surfactant for the disruption of membrane structure. It has been widely used for lysing the cells to extract protein and other cellular organelles and permeabilize the living cell membrane for transfection.[50] When Triton X-100 (0.46 mM) was mixed with the Rho-B loaded vesicular self-assemblies of ursolic acid and observed under epifluorescence microscopy at different time intervals, lysis of the spherical self-assemblies were observed (Fig. 9) confirming the vesicular nature of the spherical assemblies.

Similarly, the anionic dye CF (0.30 mM) was also entrapped inside the vesicular self-assemblies in ethanol–water (3 : 1, 30.13 mM) as observed by epifluorescence microscopy (Fig. 7c). Inspired by these results, we examined the entrapment of anticancer drug doxorubicin. A hot solution of **1** (22.93 mM) in ethanol–water (3 : 1) containing doxorubicin (0.05 mL, 2.2 mM) was cooled at room temperature and the sample was examined under epifluorescence microscopy. Reddish fluorescence observed from the vesicular self-assemblies indicated entrapment of the chemotherapeutic drug (Fig. 7d).

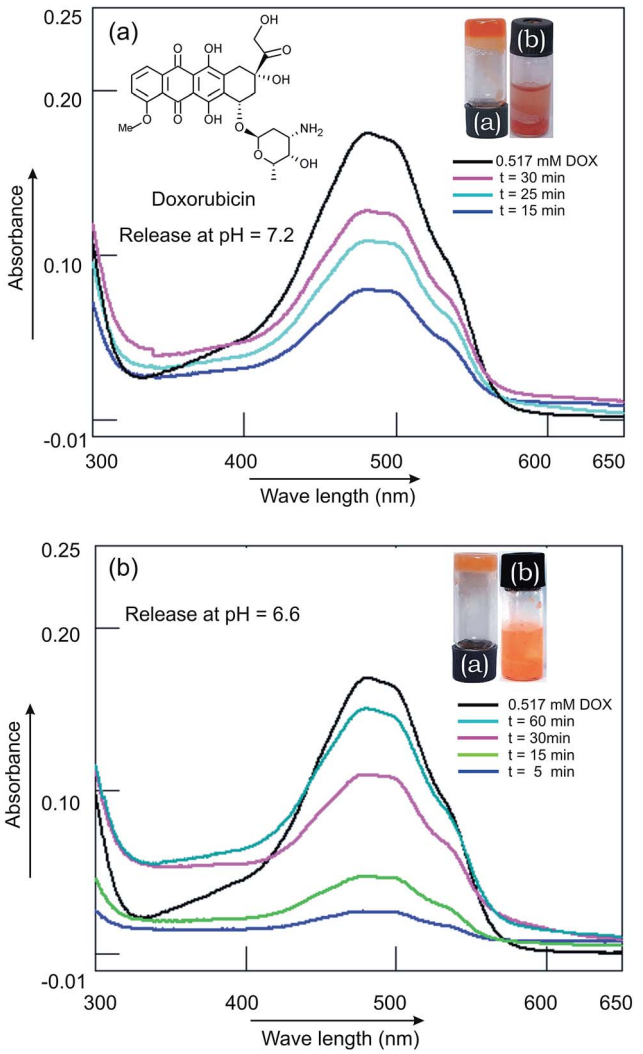


Fig. 11 Release of the ursolic acid (56.1 mM) gel-entrapped anticancer drug doxorubicin (0.51 mM) in buffer solution at (a) pH = 7.2, (b) pH = 6.6: overlay of the UV-visible spectra of the released doxorubicin to buffers at various time intervals.

### 2.5 Release study of entrapped fluorophores

Release study of the entrapped dye molecules to buffer solutions at physiological pH (7.2) is an integral part of the drug entrapment studies for prospective use of the self assemblies in drug delivery experiments.[51–54] To examine this, initially a Rho-B (0.54 mM) loaded gel of ursolic acid (54.8 mM) in DMSO–water (5 : 3, 0.16 mL) was covered with a buffer solution (10 mM, 1 mL, pH 7.2) and the release was monitored by UV-visible spectroscopy at various time intervals. Slow release of Rho-B from the Rho-B-loaded gel to the buffer solution was observed. A significant release of the Rho-B (87%) was observed after 23 h 30 min (Fig. 10). Inspired by this observation, release study of the anticancer drug doxorubicin was carried out from doxorubicin-laded gel initially at physiological pH (7.2). A doxorubicin (3.88 mM) loaded gel of ursolic acid (56.1 mM) in ethanol–water was covered with a buffer solution (10 mM, 1 mL, pH 7.2) and the release was monitored, as described before, at various time intervals. After 30 min 75% of the drug was released (Fig. 11a). Inspired by this result, we carried out the release study at a lower pH (6.6), imitating the low pH environment of hypoxic tumor or endosomes, following an identical procedure. Interestingly, the release of the anticancer drug doxorubicin at pH 6.6 was also successful (88% after 60 min, Fig. 11b) making it useful for prospective drug delivery.

## 3. Conclusions

Ursolic acid, a naturally occurring 6-6-6-6-6 ursane type monohydroxytriterpenic acid, extractable from the leaves of *Plumeria rubra* spontaneously self-assembled in organic as well as aqueous–organic liquids yielding nano-architectures such as vesicles, tubes, fibers and flowers affording supramolecular gels in many of the liquids. According to our knowledge, this is the first report of self-assembled nano-architectures from ursolic acid and the first observation of tubular self-assembly of a triterpenoid. The self-assemblies have been utilized for the entrapment of fluorophores including an anticancer drug doxorubicin. Release studies of the entrapped fluorophores including the anticancer drug doxorubicin has also been demonstrated at physiological as well as lower pH making it useful as a drug delivery vehicle.

## 4. Experimental

### 4.1 Isolation of ursolic acid 1

Finely powdered leaves of *Plumeria rubra* (16 g) were extracted with dichloromethane (300 mL) by using a Soxhlet extraction apparatus (capacity 200 mL) during 11 h. The volatiles were removed under reduced pressure to afford a yellowish solid material (1.42 g). The crude extract was purified by charcoal treatment and successive column chromatography (twice, Si-gel, 100–200 mesh, 1.2 × 12 cm) using 2–4% ethyl acetate/

dichloromethane as the eluant. The product appeared as a white solid (0.118 g, 0.73% yield).[28] Mp = 280–285 °C. FTIR (KBr, $cm^{-1}$): 3415 (w), 2930 (s), 2854 (s), 1693 (s), 1460 (s), 1392 (s), 1187 (s), 812 (s). $R_f$: 0.62 (10% ethyl acetate/dichloromethane). $^1$H NMR (400 MHz, $CDCl_3$) $\delta$: 5.18 (1H, t), 3.10 (1H, q), 2.50 (1H, d), 1.96–1.31 (20H: terpenoids proton, m). 1.19 (3H, s); 1.05 (3H, s), 1.03 (3H, d, $J = 6$ Hz), 1.02 (3H, s); 0.96 (3H, d, $J = 6$ Hz); 0.89 (3H, s); 0.86 (3H, s).

$^{13}$C NMR (150 MHz, $CDCl_3$) $\delta$: 179.5; 138.2; 125.2; 78.61; 55.18; 52.69; 47.55; 47.50; 42.02; 40.64; 40.43; 39.80; 39.59; 39.52; 38.82; 38.71; 38.59; 36.92; 32.98; 31.84; 29.60; 29.27; 28.15; 25.27; 23.71; 21.23; 17.70; 17.55; 16.48; 15.50.

MS (EI): calculated for $C_{30}H_{48}O_3$ 456.36, found 456.20.

### 4.2 Method of sample preparation and characterization

For gelation tests, ursolic acid **1** (2–5 mg) contained in a vial (1 cm id) was heated with a liquid over a hot plate with magnetic stirring until a clear solution was obtained. The solution was then allowed to cool down at room temperature (24–25 °C) and observed visually by turning the vial upside down after 2–4 h. No flow of the liquid under gravitational force indicated the formation of a gel. Samples for scanning electron microscopy were prepared by placing a dilute solution of the sample on an aluminum plate and then allowing it to dry initially in air for 24 h and then under reduced pressure for 12 h. The samples were sputter coated with Au for 165–180 s before use and studied using a Zeiss Scanning Electron Microscope (EVO 18). For optical microscopy, an aliquot of sample was placed on a glass plate and covered with a cover slip and examined using a Nikon LV100 POL microscope with D-FL Epi-fluorescence attachment. FTIR spectra of the neat powder and dried self-assemblies were analyzed by using a Perkin Elmer Spectrum Two model with KBr pellet. NMR spectra were recorded in a Bruker 400 MHz NMR and mass spectral analysis was carried out using Shimadzu Q2010 plus model. For low angle X-ray scattering experiment, a thin layer of self-assemblies of ursolic acid was taken on a glass plate and the volatiles were removed initially in air and then under reduced pressure and the diffractions were recorded in a Bruker X-ray diffractometer at 25 °C using Cu-$K_\alpha$ filament ($\lambda = 1.789$ Å). For the gel sample *m*-xylene, the gel was taken directly in the sample holder and studies. For the measurement of diffraction pattern of a powder sample, it was taken directly in the diffractometer cell and measured.

### 4.3 Entrapment studies of fluorophores

To examine whether the fluorophore rhodamine-B can be entrapped inside the vesicular self-assemblies, a hot solution of ursolic acid in ethanol–water (3 : 1, 30.13 mM) containing rhodamine B 0.30 mM was cooled at room temperature and examined by epifluorescence microscopy. Bright fluorescence from the vesicular self-assemblies indicated the entrapment of fluorophores inside the vesicles (Fig. 7a and b). When a hot solution of ursolic acid in ethanol–water (3 : 1, 30.13 mM) containing the anionic dye 5,6-carboxyfluorescein (CF) (0.30 mM) was cooled at room temperature, entrapment of the dye was observed inside the vesicular self-assemblies under epi-fluorescence microscope (Fig. 7c). Similarly, when a hot solution of ursolic acid (22.93 mM) in ethanol–water (3 : 1) containing doxorubicin (0.05 mL, 2.2 mM) was cooled at room temperature, reddish fluorescence from the vesicular self-assemblies was observed by epifluorescence microscopy indicating the entrapment of the chemotherapeutic drug (Fig. 7d).

### 4.4 Release of entrapped fluorophores into buffer solution

The Rho-B (0.54 mM) loaded gels of ursolic acid (54.8 mM) in DMSO–water (5 : 3, 0.16 mL) was covered with a phosphate buffer (10 mM, 1 mL, pH 7.2). Aliquots were carefully collected from the upper aqueous layer at various time intervals and the release of the drug was monitored by measuring the absorbance using a UV-visible spectrophotometer. After the measurement of the absorbance, the aqueous layer was carefully placed back on the top of the fluorophore-loaded gel. Significant release of the dye (87%) was observed after 23 h 30 min (Fig. 10). Release studies of doxorubicin from doxorubicin-loaded gels into buffer solutions at pH 7.2 and 6.6 were also carried out following identical procedures (Fig. 11a and b).

## Acknowledgements

We thank UGC Innovative Research, WB-DST, UGC-MRP-MAJOR-CHEM-2013-35629, UGC-SAP and DST-FIST New Delhi and Vidyasagar University for financial support and infrastructural facilities. SD, NH and ACB thank UGC for research fellowships.

## Notes and references

1 E. Carretti, M. Bonini, L. Dei, B. H. Berrie, L. V. Angelova, P. Baglioni and R. G. Weiss, *Acc. Chem. Res.*, 2010, **43**, 751–760.
2 M. Suzuki and K. Hanabusa, *Chem. Soc. Rev.*, 2009, **38**, 967–975.
3 R. G. Weiss and P. Terech, in *Molecular Gels: Materials with Self-Assembled Fibrillar Networks*, Springer, Dordrecht, 2006.
4 B. G. Bag and R. Majumdar, *Chem. Rec.*, 2017, **17**, DOI: 10.1002/tcr.201600123.
5 S. Bhattacharya and S. K. Samanta, *Chem. Rev.*, 2016, **116**, 11967–12028.
6 A. Barnard, P. Posocco, S. Pricl, M. Calderon, R. Haag, M. E. Hwang, V. W. T. Shum, D. W. Pack and D. K. Smith, *J. Am. Chem. Soc.*, 2011, **133**, 20288.
7 S. R. Jadhav, B. S. Chiou, D. F. Wood, G. D. Hoffman, G. M. Glenn and G. John, *Soft Matter*, 2011, **7**, 864.
8 K. Y. Lee and D. J. Mooney, *Chem. Rev.*, 2001, **101**, 1869.
9 S. R. Jadhav, P. K. Vemula, R. Kumar, S. R. Raghavan and G. John, *Angew. Chem., Int. Ed.*, 2010, **49**, 7695.
10 Y. Jang and J. A. Champion, *Acc. Chem. Res.*, 2016, **49**, 2188–2198.
11 D. Das, T. Kar and P. K. Das, *Soft Matter*, 2012, **8**, 2348.
12 P. Koley and A. Pramanik, *Adv. Funct. Mater.*, 2011, **21**, 4126.

 

13 M. Delample, F. Jerome, J. Barrault and J. P. Douliez, *Green Chem.*, 2011, **13**, 64.
14 B. Novales, L. Navailles, M. Axelos, F. Nallet and J. P. Douliez, *Langmuir*, 2008, **24**, 62.
15 J. P. Douliez, *J. Am. Chem. Soc.*, 2005, **127**, 15694.
16 N. Baccile, N. Nassif, L. Malfatti, I. N. A. VanBogaert, W. Soetaert, G. Pehau-Arnaudet and F. Babonneau, *Green Chem.*, 2010, **12**, 1564.
17 S. Zhou, C. Xu, J. Wang, W. Gao, R. Khverdiyeva, V. Shah and R. Gross, *Langmuir*, 2004, **20**, 7926.
18 E. Virtanen and E. Kolehmainen, *Eur. J. Org. Chem.*, 2004, **16**, 3385–3399.
19 S. Datta and S. Bhattacharya, *Chem. Soc. Rev.*, 2015, **44**, 5596.
20 H. Kobayashi, A. Friggeri, K. Koumoto, M. Amaike, S. Shinkai and D. N. Reinhoudt, *Org. Lett.*, 2002, **4**, 1423.
21 B. G. Bag, C. Garai, R. Majumdar and M. Laguerre, *Struct. Chem.*, 2012, **23**, 393.
22 S. Grassi, E. Carretti, L. Dei, C. W. Branham, B. Kahr and R. G. Weiss, *New J. Chem.*, 2011, **35**, 445.
23 B. G. Bag and S. S. Dash, *Nanoscale*, 2011, **3**, 4564.
24 B. G. Bag and S. S. Dash, *Langmuir*, 2015, **31**, 13664–13672.
25 B. G. Bag and K. Paul, *Asian J. Org. Chem.*, 2012, **1**, 150.
26 B. G. Bag and R. Majumdar, *RSC Adv.*, 2012, **2**, 8623.
27 B. G. Bag and R. Majumdar, *RSC Adv.*, 2014, **4**, 53327.
28 J. A. Silva, A. G. Silva, A. S. Alves, R. Reis, C. C. Nascimento, G. F. Diré and A. S. Barreto, *J. Med. Plants Res.*, 2013, **7**, 892–896.
29 J. Lu, X. Wu, L. Liu, H. Chen and Y. Liang, *Chem. Lett.*, 2016, **45**, 860–862.
30 D. Es-saady, A. Najid, A. Simon, A. J. Chulia and C. De-lage, *Lyon Pharm.*, 1994, **45**, 399–404.
31 H. Y. Lee, H. Y. Chung, K. H. Kim, J. J. Lee and A. W. Kim, *J. Cancer Res. Clin. Oncol.*, 1994, **120**, 513–518.
32 K. Umehara, R. Takagi, M. Kuroyanagi, A. Ueno, T. Taki and Y. J. Chen, *Chem. Bull.*, 1992, **40**, 401–405.
33 C. M. Cordero, M. Reyes, M. J. Ayuso and M. V. Toro, *Z. Naturforsch.*, 2001, **56**, 45–48.
34 J. Li, W. J. Guo and Q. Y. Yang, *World J. Gastroenterol.*, 2002, **8**, 493–495.
35 F. Lauthier, L. Taillet, P. Trouillas, C. Delage and A. Simon, *Anticancer Drugs*, 2000, **11**, 737–745.
36 H. Cha, M. T. Park, H. Y. Chung, N. D. Kim, H. Sato, M. Seiki and K. W. Kim, *Oncogene*, 1998, **16**, 771–778.
37 M. Shibuya, T. Xiang, Y. Katsube, M. Otsuka, H. Zhang and Y. J. Ebizuka, *J. Am. Chem. Soc.*, 2007, **129**, 1450.
38 B. G. Bag, P. P. Dey, S. K. Dinda, W. S. Sheldrick and I. M. Oppel, *Beilstein J. Org. Chem.*, 2008, **4**, 24.
39 N. S. Saleesh Kumar, S. Varghese, G. Narayan and S. Das, *Angew. Chem., Int. Ed.*, 2006, **45**, 6317–6321.
40 T. Rehm, V. Stepanenko, X. Zhang, F. Wurthner, F. Grohn, K. Klein and C. Schmuck, *Org. Lett.*, 2008, **10**, 1469–1472.
41 (*a*) T. Shimizu, M. Masuda and H. Minamikawa, *Chem. Rev.*, 2005, **105**, 1401–1443; (*b*) X. Huang, Y.-I. Jeong, B. Kyu Moon, L. Zhang, D. H. Kang and I. Kim, *Langmuir*, 2013, **29**, 3223–3233.
42 J. Israelachvili, *Colloids Surf., A*, 1994, **91**, 1–8.
43 (*a*) R. T. Skeel and S. N. Khleif, *Handbook of Cancer Chemotherapy*, 2011, vol. 8, pp. 1–15; (*b*) R. T. Skeel and S. N. Khleif, *Handbook of Cancer Chemotherapy*, 2011, vol. 8, pp. 45–62.
44 B. Tian, X. Tao, T. Ren, Y. Weng, X. Lin, Y. Zhang and X. Tang, *J. Mater. Chem.*, 2012, **22**, 17404.
45 P. Moitra, K. Kumar, P. Kondaiah and S. Bhattacharya, *Angew. Chem., Int. Ed.*, 2014, **53**, 1113.
46 A. Ali, M. Kamra, A. Bhan, S. S. Mandal and S. Bhattacharya, *Dalton Trans.*, 2016, **45**, 9345–9353.
47 T. Mondal, K. Dan, J. Deb, S. S. Jana and S. Ghosh, *Langmuir*, 2013, **29**, 6746–6753.
48 S. Lee, H. Chen, C. M. Dettmer, T. V. O'Halloran and S. T. Nguyen, *J. Am. Chem. Soc.*, 2007, **129**, 15096–15097.
49 S. Dinda, M. Ghosh and P. K. Das, *Langmuir*, 2016, **32**, 6701–6712.
50 (*a*) F. Gennuso, *Proc. Natl. Acad. Sci. U. S. A.*, 2004, **101**, 2470–2475; (*b*) A. Rajagopal, A. C. Pant, S. M. Simon and Y. Chen, *Cancer Res.*, 2002, **62**, 391–396.
51 Y. Nakahara, Y. Okazaki and K. Kimura, *Soft Matter*, 2012, **8**, 3192.
52 C. K. Thota, N. Yadav and V. S. Chauhan, *Sci. Rep.*, 2016, **6**, 31167.
53 Z. Luo, Y. Li, B. Wang and J. Jiang, *Macromolecules*, 2016, **49**, 6084–6094.
54 A. Baral, S. Roy, A. Dehsorkhi, I. W. Haamlay, S. Mohapatra, S. Ghosh and A. Banerjee, *Langmuir*, 2014, **30**, 929–936.